AIMETA 2019
XXIV Conference
The Italian Association of Theoretical and Applied Mechanics
Rome, Italy, 15-19 September 2019

SMART BEAM ELEMENT APPROACH FOR LRPH DEVICE

Salvatore Benfratello[1], Salvatore Caddemi[2], Luigi Palizzolo[1], Bartolomeo Pantò[2], Davide Rapicavoli[2] and Santo Vazzano[1]

[1] Department of Engineering, University of Palermo
Viale delle Scienze - 90128, Palermo, Italy
e-mail: salvatore.benfratello@unipa.it, luigi.palizzolo@unipa.it, santo.vazzano@unipa.it

[2] DICAR, University of Catania
Via Santa Sofia, 64 − 95123 Catania, Italy
scaddemi@dica.unict.it, bpanto@dica.unict.it, drapicavoli@dica.unict.it

Keywords: smart displacement, LRPH, distributed plasticity.

Abstract. *LRPH (Limited Resistance Rigid Perfectly Plastic Hinge) device is a special steel device mainly usable to join beam elements of plane or spatial steel frames covered by patent n. 102017000088597 at the Italian Ministry of Economic Development and identified in the International Patent System with the number PCT/IB2018/055766. In the framework of moment (rigid) connection, the main fundamental innovation of LRPH consists in the mutual independence of its own resistance and stiffness features. The device is constituted by a sequence of three steel elements of limited length bounded by two parallel steel plates joined up with the connected structure elements. The cross-sections of the three steel elements are classical I sections with appropriate wing and web thicknesses obtained by the solution of suitable optimal design problem. Therefore, the overall device shows piecewise discrete geometric and mechanical features. In order to implement this device in a frame-oriented code for the design of both 2D and 3D frame structures, it is necessary to adopt a suitable model based on a non-uniform cross section beam element. The latter element should be able to reproduce the elastic and plastic behavior of the device. Recently, in the literature it has been proposed a new inelastic beam element, belonging to the displacement based approach and formulated for uniform beams, based on variable displacement shape functions, whose analytic expressions are prone to updating (smart) in accordance to the plastic deformation evolution in the beam element. Aim of the paper is to utilize the relevant smart displacement beam element approach and extend it to the case of non-uniform beams to evaluate the nonlinear behavior of the LRPH device. The obtained results confirm the efficacy and the feasibility of the smart displacement beam element opening the way of implementing LRPH device in a FEM code.*

1 INTRODUCTION

The devastating effects of 1994 Northridge and 1995 Kobe earthquakes evidenced many structural problems [1-2] in several steel moment resisting frames. Following these problems, the researchers started to develop new strategies for improving the seismic performance of steel connections. Mainly, two different strategies for implementing structures able to control the behavior of column-beam joints can be found in technical and scientific literature. The first strategy (see, e.g., [3-10]) is characterized by the implementation of a connection with welded or bolted steel plates of two end tracts of beams made of steel in proximity of the beam-column joint. Aim of this strategy is to create suitable zones able to dissipate as much energy as possible. The second strategy is characterized by a reduction of the end sections of the frame beams, implementing the so-called "dog-bone" profiles, by means of cutting portions of the flanges of an I-beam profile. Such procedure substantially aims at guaranteeing to meet the required capacity design achieving, near the joint, a beam with lower resistance features than those of the column. The literature on this topic is very large (see, e.g., [11-18]), the frames equipped with this strategy are referred to as Reduced Beam Section (RBS) frames and many efforts have been performed mainly in evaluating the seismic response of RBS frames also fulfilling the so-called capacity design requirement, nowadays present in all the international standards [19-20]. Recently a new development called "double reduced beam section" has been proposed in [21] with the aim of furtherly improving the ductility behavior.

In some recent papers [22-26], some of the authors proposed an innovative device devoted to realize a new moment connection for steel elements that, from a general point of view, can be placed into the research area of reducing the beam flanges but possesses further special features as it will be described in the following. The proposed connection is a steel device, it is identified as Limited Resistance Rigid Perfectly Plastic Hinge (LRPH) and it is covered by patent n. 102017000088597 at the Italian Ministry of Economic Development and identified in the International Patent System with the number PCT/IB2018/055766. Two main ideas constitute the backbone of LRPH. The first one is that of creating a preset zone of the beam in which plastic deformations develop leaving the remaining part of the beam in the elastic range; the second one is to design the geometrical and mechanical features of the hinge in such a way that its stiffness and resistance result independent of each other and suitably selected by the designer. Further, a very important task has been that of designing a device able to minimize the cost of the post-earthquake repair. In the papers cited above LRPH is composed by three different parts: one inner and two outer. The inner one is mainly characterized by flange thickness lower than the corresponding one of the outer parts symmetrically arranged with respect to it. The mechanical model so far adopted for LRPH has been based on a rigid-perfectly plastic hinge. A more detailed model for the behavior of the device able to describe the real distribution of plastic deformations in the inner part of the LRPH device, is desirable and it will be faced in the developing of the research. A fundamental step to be performed in order to point out the applicability of LRPH in practical engineering and design regards a suitable modeling in a FEM code. To this aim the element adopted in the FEM model has to be able to correctly reproduce the main characteristics of LRPH (i.e. the geometric discontinuities and the elastic and plastic features).

The development of plastic deformations along beam elements is studied in the current practice by means of two different strategies proposed in literature: a concentrated/lumped plasticity approach and a distributed plasticity model. A comprehensive analysis and critical discussion of the two approaches is reported in [27] together with an extensive literature therein contained.

Recently in the literature [27-29] some of the authors have been involved in the formulation of elastic beam elements in presence of discontinuities by means of the use of generalised functions. The latter beam elements are able to embed different types of discontinuities along the beam span without the introduction of any additional degree of freedom.

On the basis of the latter studies, two innovative inelastic beam elements have been recently formulated in the literature [30, 31]. Both include the developments of plastic deformations by embedding generalised functions along the element span. Precisely, in [30] the onset of plastic deformations is modeled by means of Dirac's delta distributions in accordance to a concentrated plasticity approach. While in [31], within the distributed plasticity approach, the plastic deformation evolution is modeled by means of the Heaviside distribution. The latter approach, based on variable displacement shape functions, has been proposed for uniform beams. The displacement shape functions, differently from standard approaches, are prone to updating (smart) in accordance to the plastic deformation evolution. For the latter reason the beam element formulated in [31] has been addressed to as Smart Displacement Based (SDB) beam element.

In this paper, to model the presence of LRPH at the ends of beams belonging to frame systems, the attention is focused on the use of the distributed plasticity model. In particular, the Smart Displacement Based (SDB) beam element proposed in [31] is adopted and extended in order to account for the non-uniform discontinuous layout of frames when LRPH devices are employed. The extension of the SDB beam element presented in this work is adopted to evaluate the behavior of the LRPH device. A full nonlinear analysis of a frame in presence of various LRPH devices suitably placed along the frame is presented. The obtained results confirm the efficacy and the feasibility of the SDB beam element opening the way towards the implementation of LRPH device in FEM codes.

2 GEOMETRICAL AND MECHANICAL CHARACTERISTICS OF LRPH

Let us consider a typical beam element to be connected to the LRPH device, and let its cross section be inscribed into a rectangle of dimension $b \times h$ (Fig. 1(a)). Starting from this remark, the geometry of the relevant device is assumed to be inscribed in a parallelepiped of dimensions $\ell \times b \times h$ (Fig. 1(b)). The connection with the beam elements can be generally thought as a bolted plate and back-plate system assumed as a perfect rigid joint. In Fig. 1(b) bolts are not showed and the thickness of the connection plate is indicated as ℓ_p. The core of LRPH, as sketched in Figs. 1(b)-(c), is constituted by a steel element whose cross-section is characterized by a piecewise geometry, with three different portions all showing an I-shape with constant thickness. The following geometrical requirements characterize the device: a) the flanges thickness of the two outer portions is equal each other and greater than the corresponding of the inner one; b) the flanges of all the portions possess an unique common medium plane; c) the webs of the three different portions have same thickness and an unique common medium plane. By making reference to Figs. 1(a)-(c) the following geometrical characteristics are defined:

ℓ total length of the composed section;
ℓ_o common length of the outer portions;
ℓ_i length of the inner portion;
h_o common total height of the outer portions;
h_i total height of the inner portion;
t_w web thickness;
$t_{f,o}$ flange thickness of the outer portions;
$t_{f,i}$ flange thickness of the inner portion;
r welding radius between web and flanges.

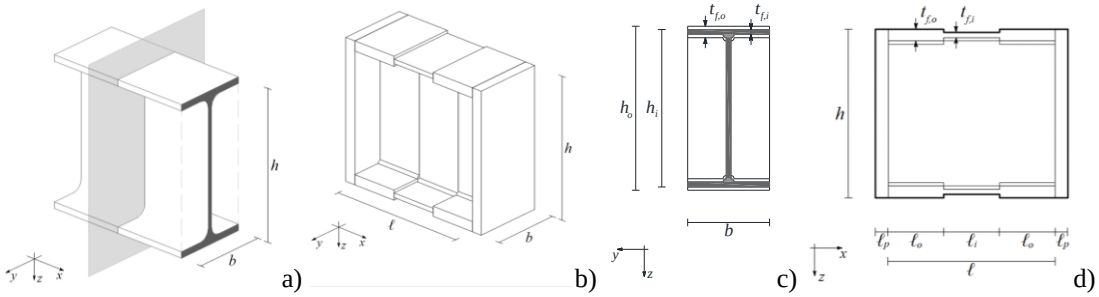

Figure 1: Sketch of LRPH device: a) Typical I-shaped steel beam element; b) 3D view; c) typical cross-section; d) lateral view.

Among the geometrical characteristics of the device reported above the welding radius r has been introduced since, from a technological point of view, the LRPH device is thought as obtained by welding of steel plates with suitable thicknesses.

For the developments of the paper, it is necessary to define the cross-section area, the moment of inertia, the elastic resistance modulus and the plastic resistance modulus, respectively, for each portion of the device. Referring to the outer portions of the LRPH these geometrical characteristics are defined by:

$$A_o = 2bt_{f,o} + t_w\left(h_o - 2t_{f,o}\right) + \pi r^2 \tag{1}$$

$$I_o = \frac{b\,t_{f,o}^3}{6} + \frac{b\,t_{f,o}}{2}\left(h_o - t_{f,o}\right)^2 + \frac{t_w\left(h_o - 2t_{f,o}\right)^3}{12} + 4r^4\left(\frac{\pi}{16} - \frac{4}{9\pi}\right) + \frac{\pi r^2}{4}\left(h_o - 2t_{f,o} - \frac{8r}{3\pi}\right)^2 \tag{2}$$

$$W_{el,o} = 2I_o/h_o \tag{3}$$

$$W_{pl,o} = b\,t_{f,o}\left(h_o - t_{f,o}\right) + t_w\left(\frac{h_o}{2} - t_{f,o}\right)^2 + \frac{\pi r^2}{2}\left(h_o - 2t_{f,o} - \frac{8r}{3\pi}\right) \tag{4}$$

The same quantities referred to the inner portion are obtained from Eqs. (1)-(4) simply substituting the geometrical characteristics with subscript "*o*" with the corresponding ones of the inner portion (subscript "*i*"). Since in this paper attention is paid only to the bending behavior of LRPH and due to assumption (see Figs. 1) that $t_{f,i} < t_{f,o}$ (which implies $W_{pl,i} < W_{pl,o}$ and $M_{pl,i} < M_{pl,o}$), the resistance limit of the device is given as follows

$$M_{pl,i} = \alpha M_{pl} = \alpha W_{pl}\sigma_0 \tag{5}$$

being α a suitably chosen scalar, W_{pl} the plastic modulus of the cross section of the connecting beam (characterized also by the flanges thickness t_p and by the moment of inertia I_p) and σ_0 the yield stress of the considered elastic-perfectly plastic material.

The main idea behind LRPH is to obtain a device substituting a portion of a beam to determine a local reduction of the limit resistance without any variation in the stiffness features. To this aim the device geometry must fulfill the following requirements: a) it becomes a perfect plastic hinge when the acting bending moment reaches a selected suitable value $M_{pl,i}$ (i.e. selecting a suitable value for $\alpha < 1$); b) for acting bending moment lower than $M_{pl,i}$ the overall elastic behavior of the device coincides to a great extent with that of the part of the beam replaced by the device; c) the overall length of the device should be the smallest as possible. The geometric parameters influencing the described requirements are mainly ℓ_o, ℓ_i, $t_{f,o}$, $t_{f,i}$. From one side, a high value of ℓ_i is desirable in order to guarantee the onset of the plastic hinge in the inner portion. From other side, in order to fulfill requirements b) it is necessary that also ℓ_o and $t_{f,o}$ possess adequate values. Finally, both ℓ_o and ℓ_i determine the overall length of the device (requirements c)). Other important remarks are that the onset of the plas-

tic hinge is strongly influenced by $t_{f,i}$ and that the lower this value the lower is that of the bending moment activating the onset. Finally, the web thickness t_w does not influence significantly the bending behavior of the device and in the numerical applications it will be assumed equal to that of the profile characterizing the connecting beam. An important remark is that, as reported in [25, 26], LRPH resistance and stiffness remain independent of each other. The above reported remarks clearly emphasize the role of ℓ_i on the correct operation of the device which has been deeply discussed in [26]. In the referenced paper it has been assumed $\ell_i = \hat{\beta}\,\overline{H}$ (being $\hat{\beta} \leq 1$ a shape ratio and $\overline{H}$ the greatest transverse dimension of the beam to be connected) and the effects of different values of $\hat{\beta}$ on the overall behavior of the LRPH have been deeply investigated, verifying that for $\hat{\beta} \geq 0.5$ the onset of the plastic hinge is ensured. As an example of the stress distribution inside the LRPH, the von Mises stress map, obtained by a suitable 3D FEM model in ABAQUS environment, in the case of an IPE 270 shape is sketched in Fig. 2. This result is obtained for an S235 steel grade, for an $\alpha = 0.8$ and $\hat{\beta} = 0.5$. An examination of this figure confirms the presence of boundary effects due to sudden change of cross section, but these effects do not influence the overall prescribed behavior of the device. Many other 3D FEM model have been analyzed considering different shapes for the cross section (for complete details on the model as well as on the results see [26]) but, for brevity's sake, they are not reported in this paper.

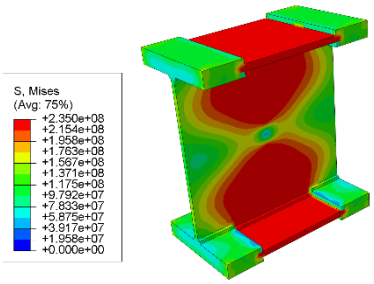

Figure 2: Von Mises stress map for IPE 270 profile, an $\alpha = 0.8$ and $\hat{\beta} = 0.5$.

3 THE SMART DISPLACEMENT BASED (SDB) BEAM ELEMENT FOR DISCONTINUOUS BEAMS

3.1 A model for discontinuous Euler-Bernoulli beams

The LRPH device, discussed in the previous section is composed of three different parts, one inner and two outers, and, for the mentioned purposes it is inserted along the axis of beam elements. The inner core is specifically designed to undergo plastic deformations. An appropriate nonlinear analysis of the latter assemblage should hence deal with beam elements characterised by cross section discontinuities and also by stiffness decay of the LRPH inner core due to the onset of plastic deformations. Along axis discontinuity of beams are usually dealt with by formulating the governing differential equations over portions of the beam and enforcing the relevant continuity conditions between adjacent segments. Alternatively, within the context of the FEM, a single FE is adopted to model each beam portion between two discontinuities. Furthermore, when a nonlinear displacement based FE approach is adopted, the adopted displacement shape functions do not account for the stiffness variations of the beam elements and are invariant with the analysis. To overcome the latter problems a preliminary mesh refinement is required or, alternatively, an a-posteriori sub-discretisation during the nonlinear analysis must be introduced. In order to provide an improvement against the mentioned beam discretisation, by avoiding any continuity condition and a sub-discretisation of discontinuous elements, some of the authors devoted attention to the study of beams with

stepped variations of the bending stiffness [32]. On the basis of the latter study the formulation of linear two node finite elements embedding different types of singularities also by adopting the classical Timoshenko theory to account for the shear deformations [31]-[32] has been also provided. However, the attention in the latter two papers was devoted to the explicit evaluation of the influence of possible discontinuities on the solution of the linear elastic problem. A full treatment of the nonlinear elastic problem of discontinuous beams is still subject under development. The evolution of the latter discontinuous two node finite elements for the nonlinear plastic analysis under the restricted hypothesis of Euler-Bernoulli beam model (by neglecting the shear deformation) has been presented in [31] where the displacement shape functions update during the analysis in accordance to the plastic deformation evolution. The latter approach is further developed in this section to embed the discontinuities due to LRPH devise along beam elements. The development herein presented, although affected by the limitation of neglected shear deformation, can be considered an intermediate step before the formulation of the model of discontinuous beam including the shear-flexural coupling nonlinear behavior. The nonlinear behavior of shear deformable beams has been modeled in literature in [33-36] where the problem related to the interaction of shear and axial stress has been studied with regard to reinforced concrete beams however in absence of discontinuities

The beam model, with along axis variable axial $E(x)A(x)$ and flexural $E(x)I(x)$ stiffness, capable of capturing the effect of stepped cross sections by means of the use of generalised functions (distributions), is adopted in this work. $E(x), A(x), I(x)$ represent the Young modulus, the area and the moment of inertia of the cross section at abscissa x spanning from 0 to the length L of the beam, respectively. The beam model under consideration is characterised by n segments with abrupt stiffness changes and can be formulated by making use of the well know Heaviside (unit step) generalised function $U(x - x_j)$, as follows:

$$E(x)A(x) = E_0A_0\left[1 - \sum_{j=1}^{n}(\beta_{x,j} - \beta_{x,j-1})U(x - x_j)\right] \tag{6a}$$

$$E(x)I(x) = E_0I_0\left[1 - \sum_{j=1}^{n}(\beta_{z,j} - \beta_{z,j-1})U(x - x_j)\right] \tag{6b}$$

In Eqs. (6), x_j indicates the abscissa along the beam axis where the *j*-th cross section change occurs, $\beta_{x,j} - \beta_{x,j-1}$ and $\beta_{z,j} - \beta_{z,j-1}$ denote the relevant axial and bending stiffness abrupt variations with respect to the reference values E_0A_0 and E_0I_0, respectively, where E_0, A_0, I_0 represent the reference values of the Young modulus, the area and the moment of inertia of the cross section, respectively. The stepped beam model introduced in Eqs. (6) implies that the beam is composed of n segments with axial stiffness E_jA_j, $j = 1, \dots, n$, assuming $\beta_{x,j} = (E_0A_0 - E_jA_j)/E_0A_0$ and flexural stiffness E_jI_j, $j = 1, \dots, n$, where $\beta_{z,j} = (E_0I_0 - E_jI_j)/E_0I_0$.

The static governing equations of the Euler-Bernoulli beam with stepped variations of the cross section depicted in Fig. 3a subjected to axial $p_x(x)$ and transversal $p_z(x)$ load distributions, in view of Eqs. (6), can be formulated as follows:

$$E_0A_0\left\{\left[1 - \sum_{j=1}^{n}(\beta_{x,j} - \beta_{x,j-1})U(x - x_j)\right]u_x'(x)\right\}' = -p_x(x) \tag{7a}$$

$$E_0I_0\left\{\left[1 - \sum_{j=1}^{n}(\beta_{z,j} - \beta_{z,j-1})U(x - x_j)\right]u_z''(x)\right\}'' = p_z(x) \tag{7b}$$

where the apex indicates the differentiation with respect to x and $u_x\ (x)$, $u_z\ (x)$ are the axial displacement and the transversal deflection functions.

Eqs. (7) can be integrated by accounting for the properties of the Heaviside generalised function and the following expressions for $u_x\ (x)$ and $u_z\ (x)$ are obtained:

$$u_x(x) = a_1 + a_2 g_2(x;\beta_{x,j}) + g_3(x;\beta_{x,j}) \tag{8a}$$

$$u_z\,(x) = c_1 + c_2 x + c_3 f_3(x;\beta_{z,j}) + c_4 f_4(x;\beta_{z,j}) + f_5(x;\beta_{z,j}) \tag{8b}$$

where the functions $g_2(x;\beta_{x,j}), g_3(x;\beta_{x,j}), f_3(x;\beta_{z,j}), f_4(x;\beta_{z,j}), f_5(x;\beta_{z,j})$ are dependent on the parameters $\beta_{x,j}$ and $\beta_{z,j}$ and are reported in the Appendix for convenience.

Eqs. (8) represent the explicit solution of the axial and transversal displacement in terms of cross section stiffness discontinuities that do not require any along axis discretisation. The latter explicit solution can hence be easily adopted for the definition of a linear finite beam element embedding the cross-section discontinuities.

However, when portions of the beam undergo plastic deformations a further variation of the axial and flexural stiffness must be accounted for during a nonlinear analysis. The same model introduced in Eqs. (6), together with the solution in Eqs. (8), may serve the latter purpose to conduct a nonlinear step-by-step analysis. In fact, the spatial evolution of the stiffness at pre-established Gauss integration points can be studied with the stepped beam model by adding further discontinuities. Furthermore, a variation of the parameters $\beta_{x,j}$ and $\beta_{z,j}$, in accordance to the tangent stiffness provided by the adopted plastic constitutive law, must be introduced. The stepped beam model, for the case of presence of LRPH at both ends of the beam, including discontinuities due to cross section variations and to stiffness decay originated by onset of plastic deformations at Gauss integration points, is depicted in Fig. 3b.

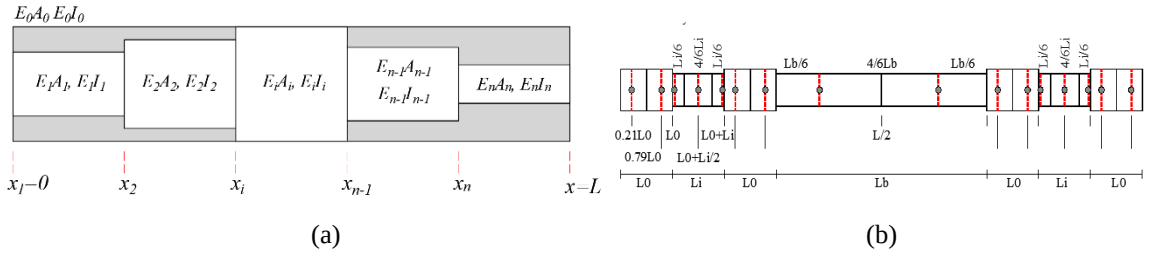

(a) (b)

Figure 3: (a) Stepped axial-flexural beam; (b) Beam element with LRPH and Gauss-control integration points.

In the next sub-section, the formulation of a nonlinear SDB beam element capable of account for plastic deformations due to both axial and transversal displacements will be presented.

3.2 The nonlinear Smart Displacement Based (SDB) beam element

A beam element, connecting joints i and j, is defined in the x,z plane as shown in Fig. 3. The nodal displacements $q_k, k = 1,\dots,6$ as in Fig. 4a, and the nodal forces $Q_k, k = 1,\dots,6$, as in Fig. 4b, are collected in the vectors $\mathbf{q}_e$, $\mathbf{Q}_e$ respectively.

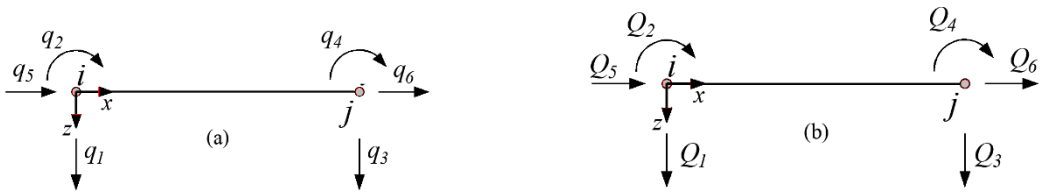

Figure 4: Nodal degrees of freedom (a) and dual forces (b) of the element.

The definition of the proposed discontinuous beam element, in accordance to the displacement based approach, is obtained by formulating the so called displacement shape functions $N_k(x), k = 1,\dots,6$, providing the contributions of unit boundary displacements to the

axial $u_x\ (x)$ and transversal $u_z\ (x)$ displacements as follows:

$$u_z\ (x) = \sum_{j=1}^{4} N_j(x;\beta_{z,j})q_j \tag{9a}$$

$$u_x\ (x) = \sum_{i=5}^{6} N_j(x;\beta_{x,j})q_j \tag{9b}$$

where the shape functions $N_k(x)$, $k = 1, \dots, 6$ have been derived by the solution in Eqs. (8) by imposing unit boundary displacements to evaluate the integration constants and are given by:

$$N_1(x;\beta_{z,j}) = 1 - \frac{f_4'(L;\beta_{z,j})}{\kappa} f_3(x;\beta_{z,j}) + \frac{f_3'(L;\beta_{z,j})}{\kappa} f_4(x;\beta_{z,j}) \tag{10a}$$

$$N_2(x;\beta_{z,j}) = x + \frac{-Lf_4'(L;\beta_{z,j}) + f_4\ (L;\beta_{z,j})}{\kappa} f_3(x;\beta_{z,j}) + \frac{-f_3\ (L;\beta_{z,j}) + Lf_3'(L;\beta_{z,j})}{\kappa} f_4(x;\beta_{z,j}) \tag{10b}$$

$$N_3(x;\beta_{z,j}) = \frac{f_4'(L;\beta_{z,j})}{\kappa} f_3(x;\beta_{z,j}) - \frac{f_3'(L;\beta_{z,j})}{\kappa} f_4(x;\beta_{z,j}) \tag{10c}$$

$$N_4(x;\beta_{z,j}) = -\frac{f_4\ (L;\beta_{z,j})}{\kappa} f_3(x;\beta_{z,j}) + \frac{f_3\ (L;\beta_{z,j})}{\kappa} f_4(x;\beta_{z,j}) \tag{10d}$$

$$N_5(x;\beta_{x,j}) = 1 - \frac{1}{g_2(L;\beta_{x,j})} g_2(x;\beta_{x,j}) \tag{10e}$$

$$N_6(x;\beta_{x,j}) = \frac{1}{g_2(L;\beta_{x,j})} g_2(x;\beta_{x,j}) \tag{10f}$$

where the external load has been neglected and the following position has been made:

$$\kappa = f_3\ (L;\beta_{z,j}) f_4'(L;\beta_{z,j}) - f_4\ (L;\beta_{z,j}) f_3'(L;\beta_{z,j}) \tag{11}$$

Eqs. (9-11) show the dependency of the displacement shape functions on the discontinuity parameters $\beta_{x,j}$ and $\beta_{z,j}$ in view of the definition of the functions $g_2(x;\beta_{x,j})$, $g_3(x;\beta_{x,j}), f_3(x;\beta_{z,j}), f_4(x;\beta_{z,j}), f_5(x;\beta_{z,j})$ as reported the Appendix.

Based on the formulation of the displacement shape function in Eqs. (10), the vector of generalised deformation components $\mathbf{d}(x) = [\varepsilon_0(x) \quad \chi_y(x)]^T$, collecting the axial deformation $\varepsilon_0(x)$ of the beam geometrical axis and the curvature $\chi_y(x)$ of the proposed plane beam element, can be expressed in terms of nodal displacements, by accounting for the standard Euler-Bernoulli model relationships, as follows:

$$\mathbf{d}(\mathrm{x}) = \mathbf{B}(\mathrm{x};\boldsymbol{\beta})\ \mathbf{q}_\mathrm{e} \tag{12}$$

where the matrix $\mathbf{B}(x;\boldsymbol{\beta})$, also dependent on the discontinuity parameters $\beta_{x,j}$ and $\beta_{z,j}$ collected in the vector $\boldsymbol{\beta}$ for conciseness, is defined in terms of derivatives of the displacement shape functions as follows:

$$\mathbf{B}(x;\boldsymbol{\beta}) = \begin{bmatrix} 0 & 0 & 0 & 0 & N_5'(x;\boldsymbol{\beta}) & N_6'(x;\boldsymbol{\beta}) \\ -N_1''(x;\boldsymbol{\beta}) & -N_2''(x;\boldsymbol{\beta}) & -N_3''(x;\boldsymbol{\beta}) & -N_4''(x;\boldsymbol{\beta}) & 0 & 0 \end{bmatrix} \tag{13}$$

During the inelastic analysis the beam element is subjected to a nonlinear state determination at suitably chosen Gauss points located at x_j^G, $j = 1, \dots, n$, where the plastic constitutive laws are integrated according to an incremental approach. The weights w_j, $j = 1, \dots, n$, associated by the integration procedure to each Gauss point, are representative of the lengths of the beam segments with decayed stiffness due to the plastic deformations.

A crucial step in the formulation of the proposed element consists in the evaluation of the stiffness variation and the consequent updating of the parameters $\beta_{x,j}$, $\beta_{z,j}$, $j = 1, \dots, n$, at each step. The displacement shape function defined in Eqs. (10) are hence subject to updating

together with the parameters $\beta_{x,j}$, $\beta_{z,j}$, $j = 1, \dots, n$, and, for this reason, they are addressed to as Smart Displacement Shape Functions (SDSF).

3.3 The element stiffness matrix by means of a fibre approach

According to a fibre approach, each Gauss cross section is discretised into n_f strips (denoted as fibres), as in Fig. 5, characterised by an area A_f, $f = 1, \dots, n_f$ and a non linear uniaxial stress- strain constitutive behaviour.

By assuming the principle of planar section conservation, and in view of Eq. (12), providing the generalised deformation component expressed in terms of nodal displacements $\mathbf{q_e}$, the axial strain $\varepsilon_x(x)$ of each fibre is written as:

$$\varepsilon_x(x; z_f) = \boldsymbol{\alpha}(z_f)\, \mathbf{B}(x; \beta_x, \beta_z)\, \mathbf{q}_e \tag{14}$$

where the row vector $\boldsymbol{\alpha}(z_f) = [1 \quad z_f]$, dependent on the distance z_f of the *f*-th fibre from the beam axis, has been introduced.

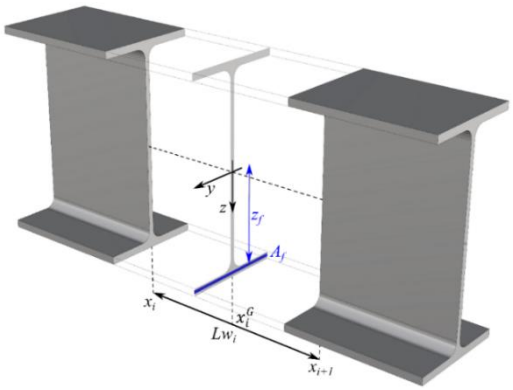

Figure 5: Fibre discretization of cross section according to a 2D formulation.

By standard application of the principle of virtual displacements, and successive adoption of the Gauss integration scheme, the element stiffness matrix $\mathbf{K}_e(\boldsymbol{\beta})$ is obtained as follows:

$$\mathbf{K}_e(\boldsymbol{\beta}) \approx L \sum_{r=1}^{n} \mathbf{B}^{\mathrm{T}}(x_r^G; \boldsymbol{\beta}) \mathbf{k}(x_r^G) \mathbf{B}(x_r^G; \boldsymbol{\beta})\, w_r \tag{15}$$

As result of the adopted SDSF, the element stiffness matrix $\mathbf{K}_\mathrm{e}(\boldsymbol{\beta})$, differently from the classical displacement-based approach commonly adopted in the literature, depends on the variation of the shape functions which are updated according to the discontinuity parameter vector $\boldsymbol{\beta}$. The inner matrix $\mathbf{k}(x)$ appearing in Eq. (15), evaluated at the Gauss cross sections, represents the cross-section stiffness matrix and is given, due to the adopted fibre discretisation, as follows:

$$\mathbf{k}(x) = \sum_{\mathrm{f}=1}^{\mathrm{n_f}} \boldsymbol{\alpha}^{\mathrm{T}}(z_f)\, E_T(x; z_f)\, A_f\, \boldsymbol{\alpha}(\mathrm{z_f}) = \begin{bmatrix} \sum_{f=1}^{n_f} E_T(x; z_f) A_f & \sum_{f=1}^{n_f} E_T(x; z_f) A_f z_f \\ \sum_{f=1}^{n_f} E_T(x; z_f) A_f z_f & \sum_{f=1}^{n_f} E_T(x; z_f) A_f z_f^2 \end{bmatrix} \tag{16}$$

The cross section stiffness matrix $\mathbf{k}(x)$ at each Gauss cross section is evaluated by performing a parallel integration of the uniaxial nonlinear constitutive laws at each fibre in the step-by-step analysis that delivers the current tangent stiffness modulus $E_T(x; z_f)$ appearing in Eq. (16). Finally, once integration of the nonlinear constitutive laws has been performed at fibre level, the updating of the discontinuity parameters $\beta_{x,j}$, $\beta_{z,j}$, $j = 1, \dots, n$, collected in

the vector $\boldsymbol{\beta}$, is obtained straightforwardly in terms of the components of the cross section stiffness matrix $\mathbf{k}(x)$ as follows:

$$\beta_{x,j} = 1 - \frac{1}{E_0 A_0}\left[\sum_{f=1}^{n_f} E_T\left(x_j^G; z_f\right) A_f + \sum_{f=1}^{n_f} E_T\left(x_j^G; z_f\right) A_f \, z_f \frac{\mathrm{d}\chi_y}{\mathrm{d}\varepsilon_0}\right] \tag{17a}$$

$$\beta_{z,i} = 1 - \frac{1}{E_0 I_0}\left[\sum_{f=1}^{n_f} E_T\left(x_j^G; z_f\right) A_f \, z_f \frac{\mathrm{d}\varepsilon_0}{\mathrm{d}\chi_y} + \sum_{f=1}^{n_f} E_T\left(x_i^G; z_f\right) A_f \, z_f^2\right] \tag{17b}$$

The step-by-step evaluation of the discontinuity parameter vector $\boldsymbol{\beta}$, in accordance to Eqs. (17), allows the updating of the SDSF in Eq. (10), the deformation matrix $\mathbf{B}(x;\boldsymbol{\beta})$ in Eq. (13) and the element stiffness matrix $\mathbf{K}_e(\boldsymbol{\beta})$ in Eq. (15). The smart character of these matrices allows the adoption of a single SDB element for each beam endowed with LRPH able to capture the diffusion of plasticity along the inner portion avoiding any cumbersome sub-discretisation.

4 APPLICATION

An important case, often faced in practical engineering, concerns the replacement of masonry panels (or portions of them) steel frames endowed with suitable stiffness. This case is focused on in this section by following the approach described in the foregoing ones. The selected case is sketched in Fig. 6 where the corresponding geometric and mechanical characteristics are also reported.

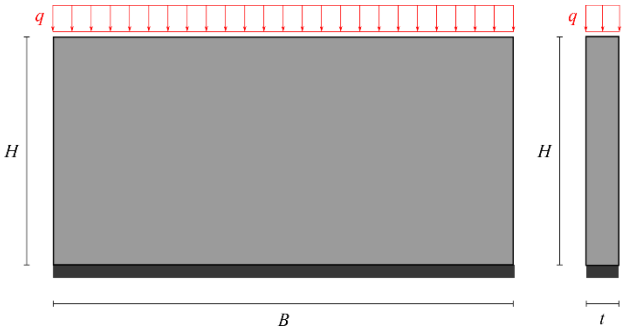

Characteristic	Value	Characteristic	Value
Width B	5.00 m	f_m	2.00 MPa
Height H	3.50 m	f_{tm}	0.10 MPa
Thickness t	0.50 m	f_{vo}	0.25 MPa
Young modulus E	1.0 GPa	Vertical load q	25 kN/m
Shear modulus G	0.4 GPa		

Figure 6: Masonry panel considered in the application.

The first performed step has been the evaluation of the push-over curve of the masonry panel reported in Fig. 6. An examination of this figure reveals that the panel shows an elastic behavior until a base shear equal to 1132 kN, while the ultimate base shear is equal to 1183 kN. From this curve it has been deduced the elastic stiffness of the masonry panel (equal to 188.60 kN/m), necessary to suitably design the equivalent steel frame. The results of this design led to IPE 750x196 and IPE 750x173 profiles for the columns and beam, respectively.

An important remark is that the limit elastic base shear and the ultimate one are very close to each other with a very flat post-elastic behavior of the push-over curve. As a consequence, it has been decided to design four LRPH devices (located at the basis of the columns and at the ends of the beam) in such a way that the four plastic hinges arise simultaneously. To this aim, the bending moments acting at the selected sections where the LRPHs are to be introduced, have been evaluated, resulting equal to 1260.00 kNm and 782.66 kNm for the column basis and the end sections of the beam, respectively. The design of LRPHs has been performed by following the optimal procedure described in [26], taking into account three different values of $\hat{\beta} = 0.3, 0.4, 0.5$, assuming $r = 0.7\, t_w$ and are reported in Table 1.

An examination of the results reported in Table 1 immediately reveals that in all the cases the overall length ℓ of each LRPH ranges between the 15% and 25% of the length of the ele-

ment in which the device has to be positioned. This remark shows many drawbacks of the actual results of the LRPH design, the main of which is that $M_{pl,i}$ is selected as the bending moment acting at the selected end of the structural element while, due to the geometric dimensions of LRPH, the inner part of the device is not close to this end. In order to avoid this drawback and taking into account that the overall stiffness of LRPH does not change if the inner part is moved at one end of the device (i.e. the LRPH shows a non-symmetric geometric outline), it has been decided to perform the analysis with SDB model in the case of non-symmetric LRPH.

	$\hat{\beta} = 0.3$		$\hat{\beta} = 0.4$		$\hat{\beta} = 0.5$	
Characteristic	Column	Beam	Column	Beam	Column	Beam
h_o	770.00	762.00	770.00	762.00	770.00	762.00
h_i	730.05	716.21	730.05	716.21	730.05	716.21
$t_{f,o}$	57.04	53.47	57.04	53.47	57.04	53.47
$t_{f,i}$	17.52	7.67	17.52	7.67	17.52	7.67
ℓ_o	113.81	269.15	151.74	358.87	189.68	448.59
ℓ_i	231.00	228.60	308.00	304.80	385.00	381.00
ℓ	458.62	766.91	611.49	1022.54	764.36	1278.18

Table 1: LRPH geometric characteristics (mm).

Once the frame equipped with LRPH has been fully characterized, it has been modeled by means of the SDB beam elements proposed in section 3 capable of embedding the geometric cross section discontinuities as well as the stiffness changes due to the nonlinear plastic behavior. The push-over curves of the frame without LRPH devices and that of the frame equipped with non-symmetric LRPH devices have been evaluated and compared with that of the masonry panel as sketched in Fig. 7. An examination of this figure allows the following remarks: a) the curves for different $\hat{\beta}$ coincide; b) the overall behavior of the frame equipped with non-symmetric LRPH is satisfactorily close to that of the masonry panel.

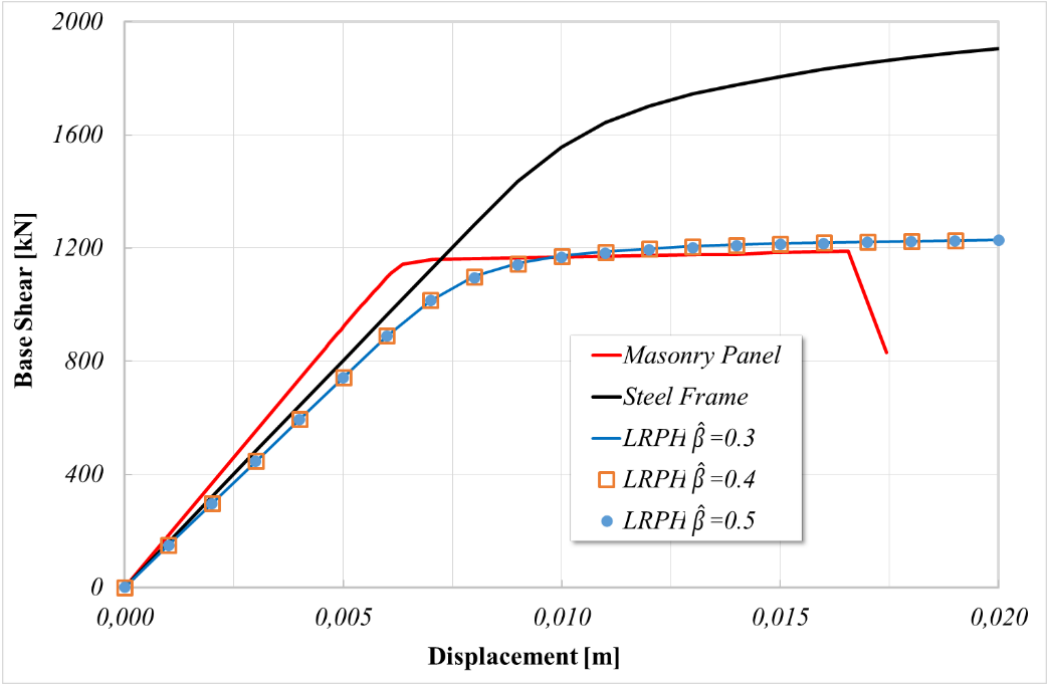

Figure 7: Comparison of the obtained results.

5 CONCLUSIONS

The present paper has been devoted to check the applicability of the distributed plasticity approach to model the presence of LRPH in frame structures. In particular, the Smart Displacement Based (SDB) beam element has been adopted and extended in order to account for the non-uniform discontinuous layout of frames when LRPH devices are employed. The proposed approach has been applied to the case of the design of a steel frame, equipped with LRPH, replacing a masonry panel with the same elastic and limit resistance of the panel. The obtained results confirm the great capacity of the LRPH device to design structures with prescribed mechanical characteristics as well as the efficacy and the feasibility of the numerical modeling by means of SDB beam elements.

AKNOWLEDGEMENTS

This work is part of the National Research Project "Advanced mechanical modelling of new materials and structures for the solution of 2020 Horizon challenges" (2017-2020), supported by MIUR, Grant No. 2015JW9NJT, Scientific coordinator, Prof. M. Di Paola, prot. n. 2015JW9NJT_017.

APPENDIX

In this Appendix the expressions of the functions $g_2(x;\beta_{x,i}), g_3(x;\beta_{x,i})$, and $f_3(x;\beta_{z,i}), f_4(x;\beta_{z,i}), f_5(x;\beta_{z,i})$, dependent on the parameters $\beta_{x,i}$ and $\beta_{z,i}$ and appearing in Equations (7a), (7b) of the main text, are reported:

$$g_2(x) = -x - \sum_{i=1}^{n}\left(\frac{\beta_{x,i}}{1-\beta_{x,i}} - \frac{\beta_{x,i-1}}{1-\beta_{x,i-1}}\right)(x-x_i)U(x-x_i)$$

$$g_3(x) = -\frac{p_x^{[2]}(x)}{E_0A_0} - \sum_{i=1}^{n}\frac{1}{E_0A_0}\left(\frac{\beta_{x,i}}{1-\beta_{x,i}} - \frac{\beta_{x,i-1}}{1-\beta_{x,i-1}}\right)\left[p_x^{[2]}(x) - p_x^{[2]}(x_i)\right]U(x-x_i)$$

$$f_3(x) = x^2 + \sum_{i=1}^{n}\left(\frac{\beta_{z,i}}{1-\beta_{z,i}} - \frac{\beta_{z,i-1}}{1-\beta_{z,i-1}}\right)(x-x_i)^2U(x-x_i)$$

$$f_4(x) = x^3 + \sum_{i=1}^{n}\left(\frac{\beta_{z,i}}{1-\beta_{z,i}} - \frac{\beta_{z,i-1}}{1-\beta_{z,i-1}}\right)[x^3 - 3x_i^2x + 2x_i^3]U(x-x_i)$$

$$f_5(x) = \frac{p_z^{[4]}(x)}{E_0J_0} + \sum_{i=1}^{n}\frac{1}{E_0J_0}\left(\frac{\beta_{z,i}}{1-\beta_{z,i}} - \frac{\beta_{z,i-1}}{1-\beta_{z,i-1}}\right)\left[p_z^{[4]}(x) - p_z^{[4]}(x_i)\right]U(x-x_i)$$
$$- \sum_{i=1}^{n}\left(\frac{\beta_{z,i}}{1-\beta_{z,i}} - \frac{\beta_{z,i-1}}{1-\beta_{z,i-1}}\right)p_z^{[3]}(x_i)(x-x_i)U(x-x_i)$$

where $p_x^{[k]}(x)$, $p_z^{[k]}(x)$ indicate the *k*-th primitive functions of the relevant external load distributions $p_x(x)$, $p_z(x)$, respectively.

REFERENCES

[1] D.K. Miller, Lessons learned from the Northridge earthquake. *Eng. Struct.*, **20** (4–6), 249-260, 1998.

[2] M. Nakashima, K. Inoue, M. Tada, Classification of damage to steel buildings observed in the 1995 Hyogoken-Nanbu earthquake. *Eng. Struct.*, **20** (4–6), 271-281, 1998.

[3] Valente M, Castiglioni CA, Kanyilmaz A. Welded fuses for dissipative beam-to-column connections of composite steel frames: Numerical analyses. *J. Constr. Steel Res.*, **128**, 498-511, 2017.

[4] Dimakogianni D, Dougka G, Vayas I. Seismic behavior of frames with innovative energy dissipation systems (FUSEIS1-2). *Engineering Structures*, **90**, 83-95, 2015.

[5] S. Wilkinson, G. Hurdman, A. Crowther, A moment resisting connection for earthquake resistant structures, *J. Constr. Steel Res.*, **62** (3), 295-302, 2006.

[6] S.S. Kumar, D.P. Rao, RHS beam-to-column connection with web opening experimental study and finite element modelling. *J. Constr. Steel Res.*, **62** (8), 739-746, 2006.

[7] C.C. Chou, K.C. Tsai, Y.Y. Wang, C.K. Jao, Seismic rehabilitation performance of steel side plate moment connections. *Earthq. Eng. Struct. Dyn.* **39** (1), 23-44, 2010.

[8] G. Dougka, D. Dimakogianni, I. Vayas, Innovative energy dissipation systems (FUSEIS 1-1) - Experimental analysis. *J. of Constructional Steel Research*, **96**, 69-80, 2014.

[9] M. Nikoukalam, K.M. Dolatshahi, Development of structural shear fuse in moment resisting frames. *J. Constr. Steel Res.* **114**, 349-361, 2015.

[10] M. Valente, C.A. Castiglioni, A. Kanyilmaz, Numerical investigations of repairable dissipative bolted fuses for earthquake resistant composite steel frames. *Eng. Struct.* **131**, 275-292, 2017.

[11] A. Plumier, Behaviour of connections. *J. of Const. Steel Res.*, **29**(1-3), 95-119, 1994.

[12] N.R. Iwankiw, C.J. Carter, The dogbone: a new idea to chew on. *Mod. Steel Constr.* **36** (4), 18-23, 1996.

[13] A. Plumier, The dogbone: back to the future. *Engineering Journal*, **34**(2), 61-67, 1997.

[14] J. Shen, T., Kitjasateanphun, W., Srivanich, Seismic performance of steel moment frames with reduced beam sections. *Engineering Structures*, **22**(8), 968-983, 2000.

[15] J. Jin, S. El-Tawil, Seismic performance of steel frames with reduced beam section connections. *Journal of Constructional Steel Research*, **61**(4), 453-471, 2005.

[16] R. Montuori, The Influence of Gravity Loads on the Seismic Design of RBS Connections. *The Open Construction and Building Techn. J.*, **8** (Suppl 1:M6), 248-261, 2014.

[17] C.E. Sofias, C.N. Kalfas, D.T., Pachoumis, Experimental and FEM analysis of reduced beam section moment endplate connections under cyclic loading. *Eng. Str.*, **59**, 320-329, 2014.

[18] S. Momenzadeh, M.T., Kazemi, M.H., Asl, Seismic Performance of Reduced Web Section Moment Connections. *Int. Journal of Steel Structures*, **17**(2), 413-425, 2017.

[19] EN 1993-1-8:2006, Eurocode 3: Design of Steel Structures Part 1-8: Design of Joints, 2006.

[20] Italian Ministry of Infrastructure and Transport, National Standard NTC 2018, DM 17/01/2018.

[21] M.A. Morshedi, K.M., Dolatshahi, S., Maleki, Double reduced beam section connection. *Journal of Constructional Steel Research*, **138**, 283-297, 2017.

[22] S. Benfratello, C. Cucchiara, L. Palizzolo, P. Tabbuso, Fixed Strength And Stiffness Hinges For Steel Frames. *Proceedings of the 23rd Conference of the Italian Association of Theoretical and Applied Mechanics (AIMETA 2017)*, Salerno, September, in Gechi Edizioni (Milano), **3**, 1287-1296, 2017.

[23] S. Benfratello, L. Palizzolo, Limited Resistance Rigid Perfectly Plastic Hinges for Steel Frames. *International Review of Civil Engineering*, **8**(6), 286-298, 2017.

[24] S. Benfratello, L. Palizzolo, P. Tabbuso, Optimal design of new steel connections. H. C. Rodrigues et al. (Eds.): *EngOpt 2018 Proceedings of the 6th International Conference on Engineering Optimization*, 644–656, 2019.

[25] S. Benfratello, L. Palizzolo, P., Tabbuso, S., Vazzano, LRPH device optimization for axial and shear stresses. *Journal of Civil Engineering and Management*, submitted to.

[26] L. Palizzolo, S. Benfratello, P. Tabbuso, S. Vazzano, On the post-elastic behaviour of LRPH connections. *Journal of Computational Design and Engineering*, submitted to.

[27] B. Biondi, S. Caddemi, Euler-Bernoulli beams with multiple singularities in the flexural stiffness. *European Journal of Mechanics A/Solids*, **26**(5), 789-809, 2007.

[28] S. Caddemi, I. Caliò, F. Cannizzaro, Closed-form solutions for stepped Timoshenko beams with internal singularities and along-axis external supports. *Archive of Applied Mechanics*, **83**, 559-577, 2013.

[29] S. Caddemi, I. Caliò, F. Cannizzaro, D. Rapicavoli, A novel beam finite element with singularities for the dynamic analysis of discontinuous frames. *Archive of Applied Mechanics*, **83**(10), 1451-1468, 2013.

[30] M.R. Hajidehi, A. Spada, G. Giambanco, The multiple slope discontinuity beam element for nonlinear analysis of RC framed structures, *Meccanica*, **53,** 1469-1490, 2018.

[31] B. Pantò, D. Rapicavoli, S. Caddemi, I. Caliò, A smart displacement based (SDB) beam element with distributed plasticity. *App. Math. Model.*, **44**, 336-356, 2017.

[32] J.P. Almeida, D. Tarquini, K. Beyer, Modelling approaches for inelastic behaviour of rc walls: Multi-level assessment and dependability of results. *Archive of Computational Methods in Engineering*, **23**, 69-100, 2016.

[33] Bentz, E. C. (2000). Sectional analysis of reinforced concrete members. Ph. D. thesis, Department of Civil Engineering, University of Toronto.

[34] Ceresa, P., L. Petrini, and R. Pinho (2007). Flexure-shear fiber beam-column elements for modeling frame structures under seismic loading—state of the art. Journal of Earthquake Engineering 11(S1), 46–88.

[35] Kagermanov, A. and P. Ceresa (2017). Fiber-section model with an exact shear strain profile for two-dimensional rc frame structures. J. of Struct. Eng. 143(10), 04017132.

[36] Vecchio, F. J. and M. P. Collins (1986). The modified compression-field theory for reinforced concrete elements subjected to shear. In J. Proc., Volume 83, pp. 219–231.